ELSEVIER

Coordination Chemistry Reviews
212 (2001) 111–131

COORDINATION CHEMISTRY REVIEWS

www.elsevier.com/locate/ccr

Applications of molecular mechanics to metal-based imaging agents

David E. Reichert, Michael J. Welch *

Mallinckrodt Institute of Radiology, Washington University School of Medicine, 510 South Kingshighway Boulevard, Campus Box 8225, Saint Louis, MO 63110, USA

Received 12 October 1999; accepted 14 April 2000

Contents

Abstract

This review summarizes some of the work done in utilizing molecular mechanics in understanding the biological behavior, and designing new ligands for the coordination of metals utilized as imaging agents in diagnostic medicine. A necessary component of this work has been the development of parameters for the commercially available modeling package SYBYL, capable of reproducing experimentally determined structures. Described in this review are our parameters for octahedral Ga(III) and In(III), Tc(V) mono-oxo complexes, and parameters for Gd(III). The second part of this review is concerned with the use of a technique known as the coordination scan which allows the determination of the sterically preferred coordination state of a metal in a given metal–ligand complex. This has proven

* Corresponding author. Tel.: +1-314-3628436; fax: +1-314-3629940.
E-mail address: welchm@mir.wustl.edu (M.J. Welch).

PII: S0010-8545(00)00367-2

extremely useful in the prediction of in vivo stability.

Keywords: SYBYL parameters; Gallium; Indium; Gadolinium; Technetium; Coordination scan

1. Introduction

Molecular modeling has found extensive use in the design of organic based pharmaceuticals and other valuable chemicals, but has not yet found wide use in the design of metal-based diagnostic agents [1,2]. Molecular modeling can be used successfully for the prediction of metal–ligand complex structure, ligand selectivity, coordination number, lipophilicity, and thermodynamic stability. In pharmaceutical development, it has become a valuable tool for QSAR (quantitative structure activity relationship) and in the development of pharmacophore models. Although not widely applied to date, it can perform these same tasks for metal-based diagnostic agents. Jurisson and co-workers [3] noted in their review on coordination compounds in nuclear medicine, 'Molecular modeling will certainly become an important aspect of the design process.'

Imaging modalities widely used in radiology include gamma scintigraphy, positron emission tomography (PET) and magnetic resonance imaging (MRI). Gamma scintigraphy requires a radiopharmaceutical containing a nuclide that emits gamma (γ) radiation and a gamma camera or single photon emission computed tomography (SPECT) camera capable of imaging the patient injected with the gamma emitting radiopharmaceutical. Positron emission tomography (PET) requires a radiopharmaceutical labeled with a positron-emitting radionuclide (β^+) and a PET camera for imaging the patient. Magnetic resonance imaging (MRI) exploits the differences in relaxation rates of water protons in tissues, translating them into three-dimensional anatomical information. Metal complexes are used in all three imaging modalities.

Molecular mechanics (MM) models of complexes of a variety of metal ions have been developed [4–8] and been shown to be useful for ligand design. Few reports exist of the use of molecular mechanics in the design and modeling of metal containing radiopharmaceuticals. Molecular modeling has perhaps been utilized the most with the complexes of the common radionuclide ^{99m}Tc [9–12]. Other metals such as Cu, Rb, Sr, and Rh that are commonly used in nuclear medicine have been studied with molecular modeling, although they were not specifically evaluated as radiopharmaceuticals [6].

We and our collaborators have developed MM parameters for the TAFF force field, found in the commercial molecular modeling package SYBYL, and techniques for modeling Ga(III) and In(III) octahedral complexes, [13,14] technetium(V) mono-oxo complexes, [15] and Gd(III) based MRI contrast agents [16]. In addition to developing force field parameters, we have furthered the application of a MM technique termed the 'coordination scan'.

2. Development of SYBYL parameters

There are three main approaches to modeling the geometry about a metal ion, these have been extensively reviewed in the past [6,8]. The valence force field (VFF) method in which all possible ligand–metal (L–M) bond lengths, and all ligand–metal–ligand (L–M–L) bond angles are defined by ideal bond angles and force constants. The points on a sphere (POS) method where the L–M bond lengths are defined with ideal values, and all L–M–L bond angles are defined by ideal bond angles. However unlike the VFF approach, no force constants are applied to L–M–L angles. The geometry about the metal center is, thus, defined solely by steric repulsions between the donor atoms. The last model is the ionic approach; the metal–ligand interaction is represented entirely with non-bonded van der Waals and electrostatic forces. Our research has focused primarily on modeling metal complexes with either the valence force field approach or the points on a sphere. To date, all of the parameter development in our lab has been for the TAFF force field found in the commercially available modeling package SYBYL [17].

2.1. Gallium and indium parameters

In(III) and Ga(III) are quite similar to each other with regard to their affinities for different donor atoms [18]. A major difference is in their ionic sizes, with In(III) being much larger [19]. There are very few reports of molecular mechanics calculations on coordination compounds of these metals in the literature. Force field parameters for bonds between N, O, and S donor atoms with both In(III) and Ga(III) were developed for six-coordinate ligands from structures found in the Cambridge Crystallographic database [14]. Due to the relatively large size of the In(III) ion, the valence force field approach was utilized in order to maintain the octahedral geometry around the ion. These parameters (Tables 1 and 2) have been used to study a variety of complexes with Ga(III) and In(III), shown in Fig. 1 [13,14]. With both types of metal complexes, the force field successfully predicted structure and relative stability.

Table 1
Bond stretching parameters for Ga(III) and In(III) in the TAFF forcefield

Bond	r_0 (Å)	Force constant (kcal mol^{-1} Å^{-2})
In–N	2.38	200
In–S	2.56	100
In–O	2.21	100
Ga–N	2.15	200
Ga–S	2.34	100
Ga–O	1.97	100

Table 2
Bond angle parameters for In(III) in the TAFF forcefield[a]

Angle	Ideal angle (°)	Force constant (kcal mol^{-1} (°) ^{2})
N–In–N	90	0.005
N–In–S	90	0.005
N–In–O	90	0.005
O–In–O	90	0.005
O–In–S	90	0.005
S–In–S	90	0.005
In–N–C	112	0.02
In–S–C	97	0.02
In–O–C	109.5	0.02

[a] The same values were used for Ga(III).

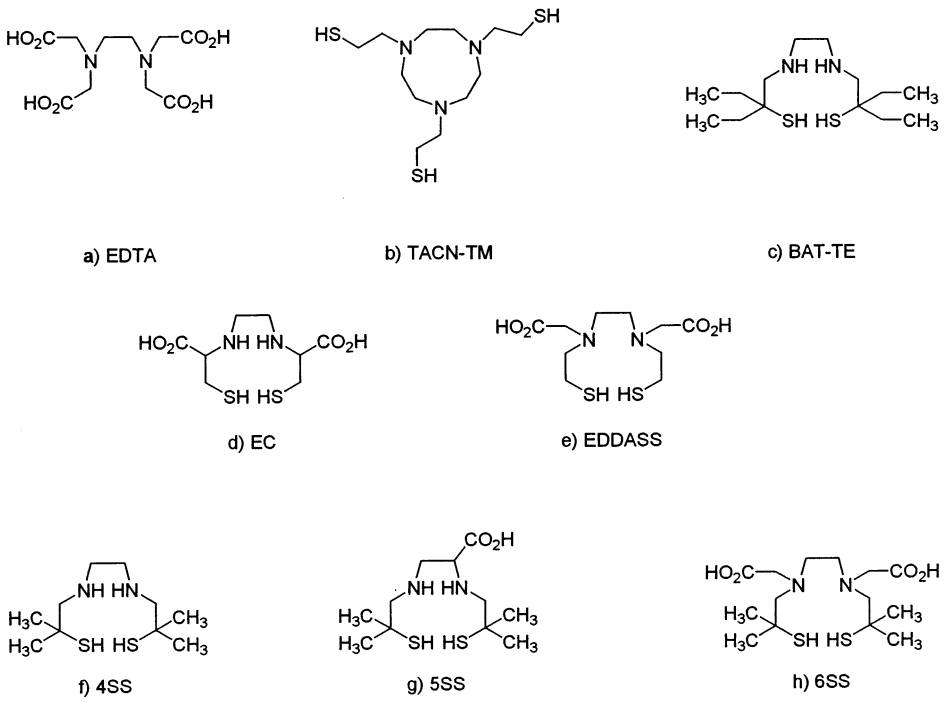

Fig. 1. Ligands for the coordination of Ga(III) and In(III).

Using *N*,*N*′-ethylenedi-L-cysteine (EC) as an example, modeling predicted that both Ga(III) and In(III) would prefer to have the sulfurs in a *cis* orientation (*cis* 8.83 kcal mol^{-1}, *trans* 13.8 kcal mol^{-1} for the Ga complex; *cis* 8.23 kcal mol^{-1}, *trans* 15.6 kcal mol^{-1} for the in complex), subsequent X-ray structures showed only the *cis* isomer [20].

2.2. Technetium(V) parameters

There are intensive efforts underway in developing technetium based radiopharmaceuticals which mimic receptor agonists or antagonists such as steroids and neuroreceptor probes [21–26]. Clearly, receptor ligands have specific stereochemical requirements, which could be prescreened with a validated molecular mechanics model of Tc complexes.

Possibly, the most common technetium complexes are those of Tc(V) with a single oxo group attached to Tc [27,28]. (see Fig. 2) The four donor atoms other than the oxo group form a square plane, with the Tc some 0.7 Å above this plane, and the Tc=O bond at a right angle to this plane. Few reports exist of molecular mechanics parameters that allow for the modeling of Tc complexes [9,29–33]. With the exception of the work by Rappé and co-workers, most of the parameters utilized are very limited in the types of complexes that can be modeled.

We undertook the development of MM parameters for Tc(V) oxo complexes with a valence force field approach. Our parameters allow for modeling TcOL4 complexes where L can be any combination of S (S of deprotonated mercaptans, or S of thioureas), the sp^2 hybridized nitrogen present in deprotonated amide nitrogens (N.am), deprotonated amine nitrogens (N.pl3), aromatic nitrogens (N.ar), sp^3 hybridized saturated nitrogen (N.4), as well as the deprotonated oxygen donor of phenols [15]. The model has been used to reproduce 35 structures of the $TcOL_4$ type. These parameters are found in Tables 3–5.

An important component of these parameters is the incorporation of fairly large torsional barriers to rotation (V_i) about the Tc–L (L, donor atom) bonds. Typi-

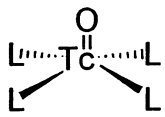

L = O, N, S

Fig. 2. Generic structure of a Tc(V) mono-oxo coordination complex.

Table 3
TAFF bond lengths for Tc(V) complexes

Bond	Bond type	r_0 (Å)	Force constant (kcal mol^{-1} $Å^{-2}$)
Tc–S	1	2.33	200
Tc–Nar	1	2.206	100
Tc–N4	1	2.2	100
Tc–Npl3	1	1.94	200
Tc–Nam	1	1.91	200
Tc–O2	2	1.65515	400
Tc–O3	1	1.96	250

cally, the torsional barriers of metal to donor atom bonds are quite small to non-existent, these large barriers are interpreted in terms of significant Tc–L π-bonding. An interpretation of Tc–L bonding that accounts for these O=Tc–L–C torsion angles is that they reflect significant overlap between filled p orbitals on the donor atoms, and d_{yz} or d_{zx} orbitals on the Tc. Zuckman et al. [34] have proposed that L to M π-bonding is important in the Tc–L bonds of square pyramidal complexes of the Tc(V)O group. In support of the π-bonding interpretation, the need for torsional constants of this type arises only for donor atoms with filled p-orbitals suitable for L–M π-bonding, such as thiol S, deprotonated amide nitrogen, or phenolic oxygen.

2.3. Gadolinium parameters

Current MRI contrast agents in clinical use are polyamino carboxylate complexes of gadolinium, i.e. MAGNEVIST (GdDTPA, Berlex Laboratories), OMNISCAN (GdDTPA-BMA, Nycomed), ProHance (GdHP-DO3A, Squibb) and DOTAREM (GdDOTA, Guerbet). The structures of these ligands are shown in Fig. 3. A key requirement for a potential gadolinium containing contrast agent is a high in vivo stability towards dissociation, as free Gd(III) is highly toxic and retained in the liver, spleen, and bone [35]. Cacheris and co-workers [36] have found that high thermodynamic stability doesn't ensure low toxicity, rather the ligand utilized must be selective towards Gd^{3+} over the endogenous ions Zn^{2+}, Cu^{2+}, Fe^{3+} and Ca^{2+}.

Parameters for modeling Gd(III) complexes have been reported for several force fields over the years. Fossheim and co-workers utilized the AMBER force field to examine several Gd based MRI contrast agents [37–39]. Parameters for the MM2 and MM3 force fields for Gd(III) have been reported by several groups [40–42]. Rappé's universal force field (UFF) also contains parameters for modeling Gd [43]. As with the previously discussed metals, we developed parameters (see Table 6) for the TAFF force field utilized in SYBYL [16]. A more recent set of TAFF parameters has recently been published [44].

The Gd(III) parameters we developed were derived from a total of twelve gadolinium complex structures. The most critical parameter found to affect the metal complex structures was the equilibrium bond length between the gadolinium and donor atoms. The parameters derived from these was found to reproduce the crystal structures reasonably well (average positional rms, 0.3624 Å). In all cases, the effects of electrostatics were ignored so that the metal complex structure is determined solely by steric effects.

3. The 'coordination scan'

Hancock and co-workers [5] have utilized molecular mechanics to determine the relationship between ligand selectivity and metal ion size. The technique utilized in these studies is the calculation of the complex strain energy as a function of the M–L bond length. This is accomplished by modeling the complex with a generic

Table 4
TAFF angle definitions for Tc(V) complexes

Atom 1	Atom 2	Atom 3	Equil. angle (°)	Force constant (kcal mol^{-1} (°)^2)
O.2	Tc.5	S.3	109.1	0.008
S.3	Tc.5	S.3	141.8	0.008
S.3	Tc.5	S.3C	84	0.008
S.3C	Tc.5	S.3C	141.8	0.008
O.2	Tc.5	S.3C	109.1	0.008
ANY	S.3	Tc.5	105.9	100
ANY	S.3C	Tc.5	105.9	100
C.3	S.3	Tc.5	98	0.008
C.3	S.3C	Tc.5	98	0.008
C.ar	S.3	Tc.5	98	0.008
C.ar	S.3C	Tc.5	98	0.008
C.2	S.3	Tc.5	105.9	0.008
C.2	S.3C	Tc.5	105.9	0.008
S.3	C.2	S.3C	120	0.008
N.4	Tc.5	N.4	180	0.008
N.4	Tc.5	S.3	150	0.008
N.4	Tc.5	N.4T	85.1	0.008
N.4T	Tc.5	S.3C	150	0.008
N.4	Tc.5	O.2	110	0.008
N.4T	Tc.5	O.2	110	0.008
N.4	Tc.5	S.3C	82.8	0.008
N.4T	Tc.5	S.3	82.8	0.008
N.pl3	Tc.5	S.3	129	0.008
N.pl3	Tc.5	S.3C	82.8	0.008
N.4T	Tc.5	N.pl3	82.8	0.008
N.pl3	Tc.5	O.2	117.8	0.008
N.4T	Tc.5	N.4T	150	0.008
N.pl3	Tc.5	N.pl3	150	0.008
N.pl3B	Tc.5	S.3C	150	0.008
N.pl3B	Tc.5	S.3	82.8	0.008
N.pl3B	Tc.5	O.2	117.8	0.008
N.pl3	Tc.5	N.pl3B	80	0.008
N.am	Tc.5	S.3	150	0.008
N.amC	Tc.5	S.3C	150	0.008
N.am	Tc.5	O.2	109.1	0.008
N.amC	Tc.5	O.2	109.1	0.008
N.am	Tc.5	N.amC	81.2	0.008
N.am	Tc.5	S.3C	82.1	0.008
N.amC	Tc.5	S.3	82.1	0.008
N.4T	Tc.5	N.pl3B	150	0.008
N.ar	Tc.5	N.pl3	150	0.008
N.ar	Tc.5	S.3C	82.8	0.008
N.pl3B	Tc.5	N.pl3B	150	0.008
O.3	Tc.5	O.3	142	0.008
O.3	Tc.5	O.3C	81.9	0.008
O.2	Tc.5	O.3	108.9	0.008
O.2	Tc.5	O.3C	108.9	0.008
O.3C	Tc.5	O.3C	142	0.008
N.am	Tc.5	N.pl3	140	0.008

Table 4 (Continued)

N.amC	Tc.5	N.pl3B	140	0.008
N.amC	Tc.5	N.pl3	77.4	0.008
N.am	Tc.5	N.pl3B	77.4	0.008
N.4T	Tc.5	N.am	81	0.008
N.4	Tc.5	N.amC	81	0.008
N.4	Tc.5	N.am	142	0.008
N.4T	Tc.5	N.amC	142	0.008

metal while varying its ionic radius, the resultant curves give a minimum energy which corresponds to the best-fitting metal ion radius. An example of such a scan is shown in Fig. 4 for the ligand 4SS (Fig. 1(f)), the minima of the energy curve occurs at ca. 0.65 Å, suggesting the best fit to an ion of this size.

A related technique is the 'coordination scan', in which a series of curves are generated by minimizing complexes with various numbers of water molecules coordinated to the metal ion while changing the M–L bond lengths [45]. Such curves serve to indicate the steric strain induced on the ligand by binding additional coordinating ligands (water) onto the metal ion. An important point to note is that SYBYL calculates water as having a strain energy of 0.00 kcal mol^{-1}, thus, the waters added to the complex add no energy other than steric interactions with the ligand. Examination of the intersection points for these curves, as well as to which side of this point the preferred ionic radius for the metal ion in a given coordination state falls, indicates the preferred coordination number. At the same time, the curves also show the ligand selectivity based on ionic size.

3.1. Gallium and indium complexes

Molecular modeling was applied to the Ga(III) and In(III) complexes of the ligands shown in Fig. 1, in order to understand their structures and in vivo stabilities [13]. The initial step was to determine the preferred coordination of each complex, as this determines the geometry about the metal. Ga(III) is typically found as four-, five-, or six-coordinate while In(III) prefers four, six, or eight coordination.

Using the coordination scan, each complex was made four-, five-, six-, and eight-coordinate by the addition of water molecules to the metal ion, the metal's ionic radius was allowed to range from 0.3 to 1.5 Å [19]. This accounts for the preferred coordination numbers and ionic radii for both Ga and In. An example of one of these scans, the ligand 4SS (Fig. 1(f)), is shown in Fig. 5 with the preferred ionic radii for both Ga(III) and In(III) indicated.

In Fig. 5 we see that the intersection point for four- and five-coordinate species occurs at approximately 0.35 Å, the ionic radii for four-coordinate Ga(III) is 0.47 Å while that of five-coordinate Ga(III) is 0.55 Å. Since the four-coordinate radius is past the intersection point, it may be concluded that the complex prefers to be five-coordinate. A similar analysis of the five- and six-coordinate intersection point (ca. 0.4 Å) shows that the preferred five-coordinate radius lies past the intersection

Table 5
TAFF torsion definitions for Tc(V) complexes

Atom 1	Atom 2	Atom 3	Atom 4	Bond type	Force constant (kcal $mol^{-1}Å^{-2}$)	Periodicity
C.3	S.3	Tc.5	ANY	1	0	0
C.3	S.3C	Tc.5	ANY	1	0	0
ANY	ANY	Tc.5	ANY	1	0	0
C.3	S.3C	Tc.5	S.3	1	0	0
C.3	S.3C	Tc.5	S.3C	1	0	0
C.3	S.3	Tc.5	S.3	1	0	0
C.3	S.3	Tc.5	S.3C	1	0	0
C.3	S.3	Tc.5	O.2	1	2	2
C.3	S.3C	Tc.5	O.2	1	2	2
ANY	S.3	Tc.5	O.2	1	0	3
ANY	S.3C	Tc.5	O.2	1	0.3	2
Tc.5	S.3C	Tc.5	S.3	1	0	3
Tc.5	S.3C	Tc.5	S.3C	1	0	3
Tc.5	S.3C	Tc.5	O.2	1	0	3
Tc.5	S.3	Tc.5	S.3	1	0	3
Tc.5	S.3	Tc.5	O.2	1	0	3
Tc.5	S.3	Tc.5	S.3C	1	0	3
C.2	S.3	Tc.5	S.3	1	0	3
C.2	S.3	Tc.5	S.3C	1	0	3
C.2	S.3	Tc.5	O.2	1	3.5	2
C.ar	S.3	Tc.5	O.2	1	3.5	2
C.ar	S.3C	Tc.5	O.2	1	3.5	2
C.ar	S.3C	Tc.5	S.3	1	0	3
C.ar	S.3	Tc.5	S.3	1	0	3
C.ar	S.3	Tc.5	S.3C	1	0	3
C.3	C.3	S.3	Tc.5	1	0	3
C.3	C.3	S.3C	Tc.5	1	0	3
C.2	S.3C	Tc.5	O.2	1	3.5	2
C.3	N.3T	Tc.5	O.2	1	0	3
C.3	N.4	Tc.5	O.2	1	0	3
C.3	N.4	Tc.5	S.3	1	0	3
C.3	N.4	Tc.5	N.4T	1	0	3
C.3	N.4	Tc.5	S.3C	1	0	3
H	N.4T	Tc.5	O.2	1	0	3
H	N.4T	Tc.5	S.3	1	0	3
H	N.4T	Tc.5	S.3C	1	0	3
H	N.4T	Tc.5	N.4	1	0	3
C.3	N.4T	Tc.5	S.3	1	0	3
C.3	N.4T	Tc.5	S.3C	1	0	3
C.3	N.4T	Tc.5	N.4	1	0	3
C.3	N.4T	Tc.5	O.2	1	0	3
C.3	S.3	Tc.5	N.4	1	0	3
C.3	S.3C	Tc.5	N.4T	1	0	3
C.3	S.3	Tc.5	N.4T	1	0	3
C.3	N.pl3	Tc.5	O.2	1	3.5	2
C.3	N.pl3	Tc.5	S.3	1	0	3
C.3	N.pl3	Tc.5	S.3C	1	0	3
C.3	N.pl3	Tc.5	N.4T	1	0	3

Table 5 (Continued)

C.3	S.3	Tc.5	N.pl3	1	0	3
C.3	S.3C	Tc.5	N.pl3	1	0	3
C.3	N.4T	Tc.5	N.pl3	1	0	3
H	N.4T	Tc.5	N.4T	1	0	3
C.3	N.4T	Tc.5	N.4T	1	0	3
H	N.4	Tc.5	N.4	1	0	3
C.3	N.4	Tc.5	N.4	1	0	3
H	N.4	Tc.5	O.2	1	0	3
H	N.4	Tc.5	N.4T	1	0	3
C.3	N.pl3	Tc.5	N.pl3	1	0	3
H	N.4T	Tc.5	N.pl3	1	0	3
C.3	N.pl3B	Tc.5	O.2	1	3.5	2
C.2	N.pl3B	Tc.5	O.2	1	3.5	2
C.3	S.3C	Tc.5	N.am	1	0	3
C.3	S.3C	Tc.5	N.amC	1	0	3
C.3	S.3	Tc.5	N.am	1	0	3
C.3	S.3	Tc.5	N.amC	1	0	3
C.3	N.am	Tc.5	S.3	1	0	3
C.3	N.am	Tc.5	S.3C	1	0	3
C.3	N.am	Tc.5	N.amC	1	0	3
C.2	N.am	Tc.5	S.3	1	0	3
C.2	N.am	Tc.5	S.3C	1	0	3
C.2	N.am	Tc.5	O.2	1	3.5	2
C.2	N.amC	Tc.5	O.2	1	3.5	2
C.3	N.am	Tc.5	O.2	1	3.5	2
C.3	N.amC	Tc.5	O.2	1	3.5	2
C.2	N.am	Tc.5	N.amC	1	0	3
C.2	N.amC	Tc.5	N.am	1	0	3
C.ar	N.pl3	Tc.5	O.2	1	3.5	2
C.ar	N.pl3B	Tc.5	O.2	1	3.5	2
C.ar	N.pl3	Tc.5	N.pl3B	1	0	3
C.ar	N.pl3B	Tc.5	N.pl3	1	0	3
C.3	N.pl3	Tc.5	N.pl3B	1	0	3
C.3	N.pl3B	Tc.5	N.pl3	1	0	3
C.ar	N.pl3	Tc.5	S.3	1	0	3
C.ar	S.3	Tc.5	N.pl3B	1	0	3
C.ar	N.pl3	Tc.5	S.3C	1	0	3
C.ar	S.3	Tc.5	N.pl3	1	0	3
C.3	S.3	Tc.5	N.pl3B	1	0	3
C.3	N.4T	Tc.5	N.pl3B	1	0	3
C.ar	N.am	Tc.5	O.2	1	3.5	2
C.ar	N.amC	Tc.5	O.2	1	3.5	2
C.ar	N.am	Tc.5	S.3	1	0	3
C.ar	N.am	Tc.5	S.3C	1	0	3
C.ar	N.am	Tc.5	N.amC	1	0	3
C.ar	S.3	Tc.5	N.am	1	0	3
C.ar	S.3C	Tc.5	N.amC	1	0	3
C.ar	S.3	Tc.5	N.amC	1	0	3
C.ar	N.amC	Tc.5	N.am	1	0	3
H	N.pl3	Tc.5	N.pl3B	1	0	3
H	N.pl3B	Tc.5	N.pl3	1	0	3
H	N.pl3	Tc.5	N.pl3	1	0	3

Table 5 (Continued)

C.ar	N.pl3	Tc.5	N.pl3	1	0	3
H	N.pl3	Tc.5	O.2	1	0	3
C.ar	O.3	Tc.5	O.2	1	3.5	2
C.ar	O.3C	Tc.5	O.2	1	3.5	2
C.ar	O.3C	Tc.5	O.3C	1	0	3
C.ar	O.3C	Tc.5	O.3	1	0	3
C.ar	O.3	Tc.5	O.3C	1	0	3
C.ar	O.3	Tc.5	O.3	1	0	3
O.2	C.2	S.3	Tc.5	1	6	−2
O.2	C.2	S.3C	Tc.5	1	6	−2
O.3	N.am	Tc.5	O.2	1	3.5	2
O.3	N.amC	Tc.5	O.2	1	3.5	2
C.3	N.pl3	Tc.5	N.amC	1	0	3
C.3	N.pl3	Tc.5	N.am	1	0	3
Tc.5	N.amC	O.3	H	1	0	3
O.3	N.am	Tc.5	N.pl3	1	0	3
C.2	N.am	Tc.5	N.pl3	1	0	3
C.2	N.am	Tc.5	N.pl3B	1	0	3
O.3	N.am	Tc.5	N.pl3B	1	0	3
O.3	N.amC	Tc.5	N.am	1	0	3
O.3	N.am	Tc.5	N.amC	1	0	3

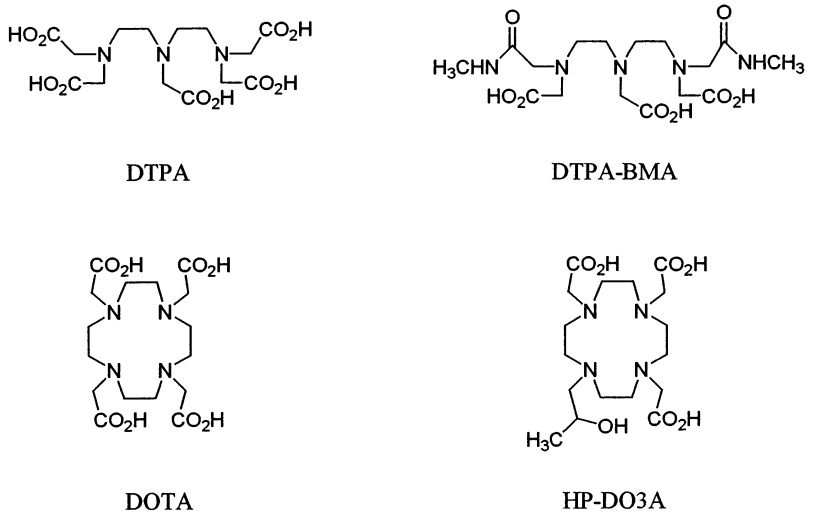

Fig. 3. Amino carboxylate ligands used for coordinating Gd(III) in commercially available MRI contrast agents.

point, as does the preferred ionic radius for six-coordinate Ga(III) 0.62 Å. The coordination scan, therefore, indicates that the Ga(III) complex would prefer to bind two water molecules raising the coordination number of the metal to six. A similar analysis for In(III) leads to a predicted coordination number of six also.

Table 6
Gd parameters for TAFF

Gd–L	Bond type	Equal length (Å)			Force constant (kcal mol^{-1} Å^{-1})	
Bond length parameters						
L=N sp^{-2}	1	2.616			100	
N secondary	1	2.68			100	
N tertiary	1	2.695			100	
N sp^2 aromatic	1	2.630			100	
O sp^2	1	2.420			100	
O sp^3	1	2.397			100	
Angle definition		Equal angle (deg)				
Angle parameters						
–Gd–		90			0	
Atom 1	Atom 2	Atom 3	Atom 4	Type		Periodicity
Torsion parameters						
O sp^2	C sp^2	O sp^3	Gd	1	1	−2
C sp^3	C sp^2	O sp^3	Gd	1	1	−2

A summary of these calculations is found in Table 7, as well as the in vivo serum stability at 1 h. The modeling studies suggest that stability in the presence of other ligands, as is the case in biological systems, depends on the complex leading to a favored coordination state. Complexes where the ligand fulfills the coordination requirements of the metal will be more stable than those where the metal is left with vacant coordination sites. As is seen in Table 7, complexes of both In(III) and

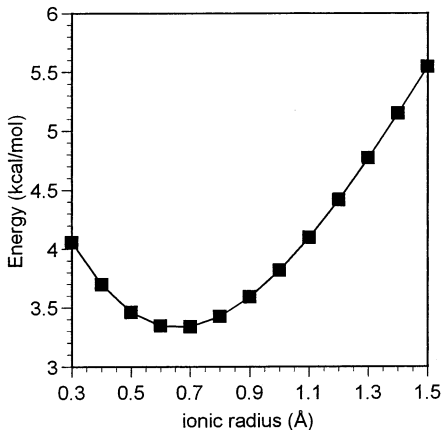

Fig. 4. A metal size ligand fit plot for the ligand 4SS.

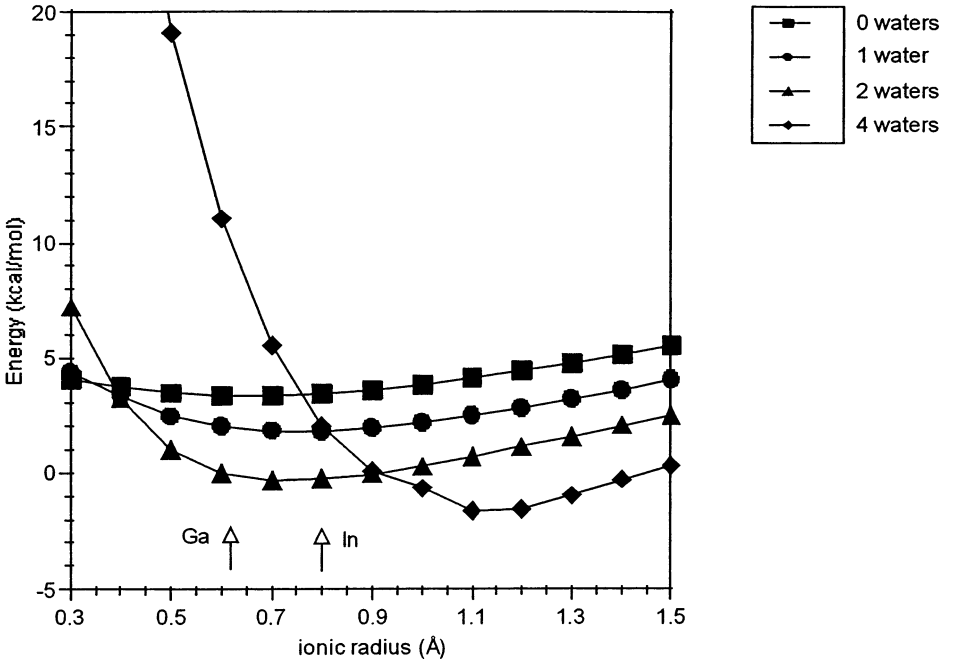

Fig. 5. Coordination scan for the ligand 4SS with the preferred ionic radii of six-coordinate Ga(III) (0.62 Å) and six-coordinate In(III) (0.80 Å). Both metal complexes are predicted to bind an additional two ligands.

Table 7
Predicted coordination number and in vivo stability at 1 h

Ligand	Predicted coordination number		Serum stability at 1 h[a]	
	Ga	In	Ga	In
4SS	6	6	25	2
5SS	5	6	19	19
6SS	6	6	100	100

[a] Reported as percent intact complex.

Ga(III) with 4SS and 5SS will prefer to bind additional ligands, and show a significantly lower stability than those formed with 6SS.

Another study where the coordination scan proved invaluable involved the ligand tris(2-mercaptobenzyl)amine (NS3); the structure is shown in Fig. 6. This ligand was originally designed to model the active site of metalloproteins by Koch and co-workers [46]. Initial modeling studies indicated that this ligand would be suitable for labeling with gallium and possibly indium. We found that the Ga(III) and In(III) complexes of this ligand displayed interesting biological behavior, including

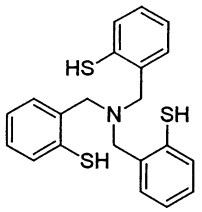

NS3

Fig. 6. Structure of the ligand NS3.

crossing of the blood–brain barrier by the Ga(III) complex [47]. Fig. 7 shows the coordination scan of NS3, which is capable of forming a four-coordinate complex with both Ga and In.

The coordination scan indicated that this ligand would bind both Ga(III) and In(III); however several differences were predicted between the complexes formed by these two metals. The Ga(III) complex was predicted to be four-coordinate, thus the ligand fulfills the coordination requirements of the metal. The In(III) complex was predicted to favor a five-coordinate complex. Indeed these predictions were

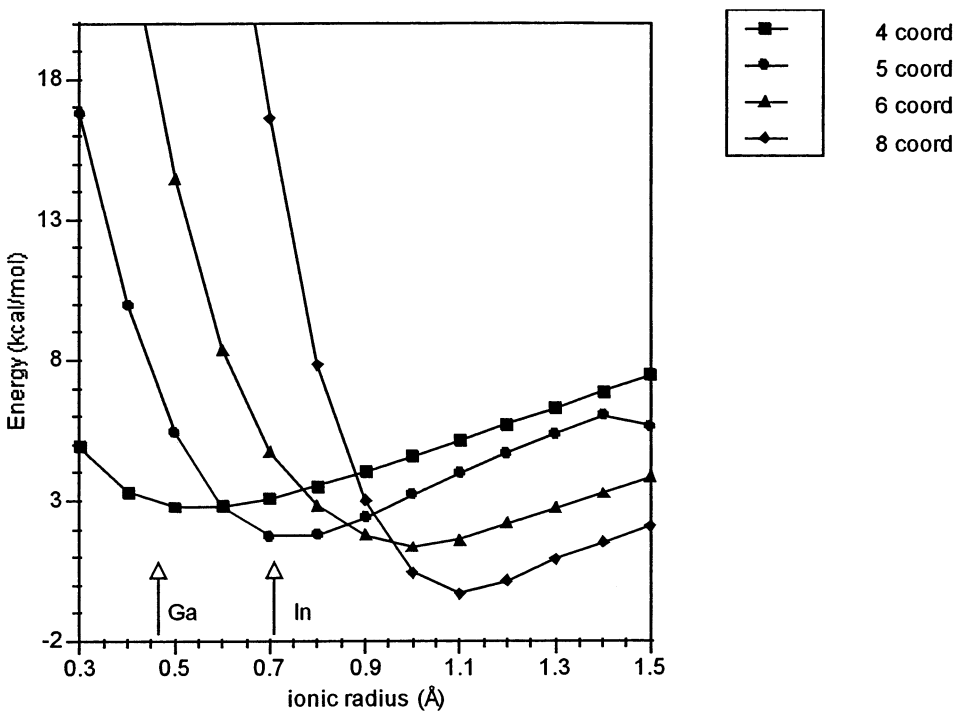

Fig. 7. Coordination scan for the ligand NS3 with the preferred ionic radii of four-coordinate Ga(III) (0.47 Å) and five-coordinate In(III) (0.705 Å).

Table 8
Comparison of the coordination scan with X-ray structures

Ligand	Predicted coordination number			Actual coordination number		
	Ga	In	Reference	Ga	In	Reference
TACN-TM	6	6	[14]	6	6	[51,52]
EC	6	6	[14]	6	6	[20]
NS3	4	5	[47]	4	5	[48]

Table 9
Coordination scan compared to experimental determination of q

Complex	Predicted q	Experimental q	Reference
GdEDTA	3	3	[53]
GdDTPA	1	1	[54]
GdDTPA-BMA	1	1	[55]
GdDTPA-BEA	1	1	[56]
GdDTPA-BPA	1	1 (NMR)	[57]
GdBOPTA	1	1	[58]
GdDOTA	1	1	[59]
GdDO3A	2	1.8 (lum.)	[59]
GdDO3MA	2	2	[60]
GdDOTA-OH	1	1	[61]
GdHP-DO3A	1	1	[62]
GdHAM2	3	3	[63]

later born out with subsequent determination of the complexes crystal structures, the GaNS3 complex was found to be four-coordinate, and InNS3 was found to be five-coordinate with the fifth coordination site being filled by a DMF molecule coordinated through the carbonyl oxygen [48]. Table 8 compares the results of the coordination scan to crystallographic data.

3.2. Gadolinium complexes

In an attempt to develop tools useful in designing new MRI contrast agents, we applied the coordination scan to determine the coordination number of Gd in most of the complexes reported in the literature [16]. Ideally, these scans would allow for the prediction of the number of waters bound to the Gd (q), which relates to the overall relaxivity, as well as an estimation of the complex's thermodynamic stability.

An initial complex structure was generated from X-ray coordinates whenever possible. The Gd in each complex was, then, adjusted to the different coordination numbers by covalently binding the appropriate number of waters to the metal. The ionic radius was varied from 0.5 to 1.5 in 0.1 Å increments, in order to cover the radii of all the possible coordination states [19]. This procedure was, then, repeated

for the complex with one water, two waters, and so on, until all the possible coordination states were examined.

Plots of the complex energy versus metal ionic radius were, then, generated for each coordination number. These curves were, then, fit to third order polynomial of the form $y = ax^3 + bx^2 + cx + d$, and the resultant curves plotted together. The curve equations can, then, be solved simultaneously in order to determine the intersection points, or 'crossover points'. Examination of the position of these crossover points in relation to the preferred ionic radius for the metal ion in a given coordination state indicates the preferred coordination number. For Gd^{3+} the radius for a six-coordinate environment is 0.938, for seven-coordinate, it is 1.00, for eight- 1.053, and for nine-coordinate 1.107 Å [19].

In order for a given coordination state to be favorable, the preferred ionic radius must be on the correct side of the crossover point, the closer an ionic radius is to a crossover point, the more the other coordination state contributes to the equilibrating system. In addition, the energy difference between the 'ideal radii' of a particular coordination number and the crossover point indicates how readily the coordination of a particular complex will change; a small difference in energies is favorable, while a large difference would disfavor a change in coordination.

The 'coordination' scan allows the determination of the coordination number and thus q, it also helps to determine the molecular weight of the solvated complex which is important for the rotational motion. This technique appears to be quite successful in predicting the number of waters bound to the Gd, as seen in Table 9. The results for GdEDTA, GdDTPA, GdDTPA-BMA, GdDTPA-BEA, GdDTPA-BPA, GdBOPTA, GdDOTA, GdDO3A, GdDO3MA, and GdHP-DO3A all match the experimental q values found in the literature.

An intriguing observation has been made through the use of the coordination scan. The energy difference ΔE_{coord}, between the solvated complex, with the appropriate number of waters bound to the Gd, and the desolvated complex correlates to the thermodynamic stability constant log K. This energy difference represents the energetic cost in changing the coordination state of a complex from the preferred state, including solvation, to that due entirely to the coordinating ability of the ligand alone. A remarkable feature of this is that this effect is due entirely to steric interac-

Table 10
Experimentally determined stability constants and ΔE_{coord}

Ligand	log K	ΔE_{coord} (kcal mol^{-1})
MCTA	27	1.6155
DOTA-OH	25.9	1.3333
DOTA	24	2.4510
HP-DO3A	23.8	3.8023
DTPA	22.39	3.1546
L-DTPA	21.99	5.4967
DTTAP	19.74	5.7760
CPDTA	18.22	8.9999
BDTA *cis*	17.03	8.9004

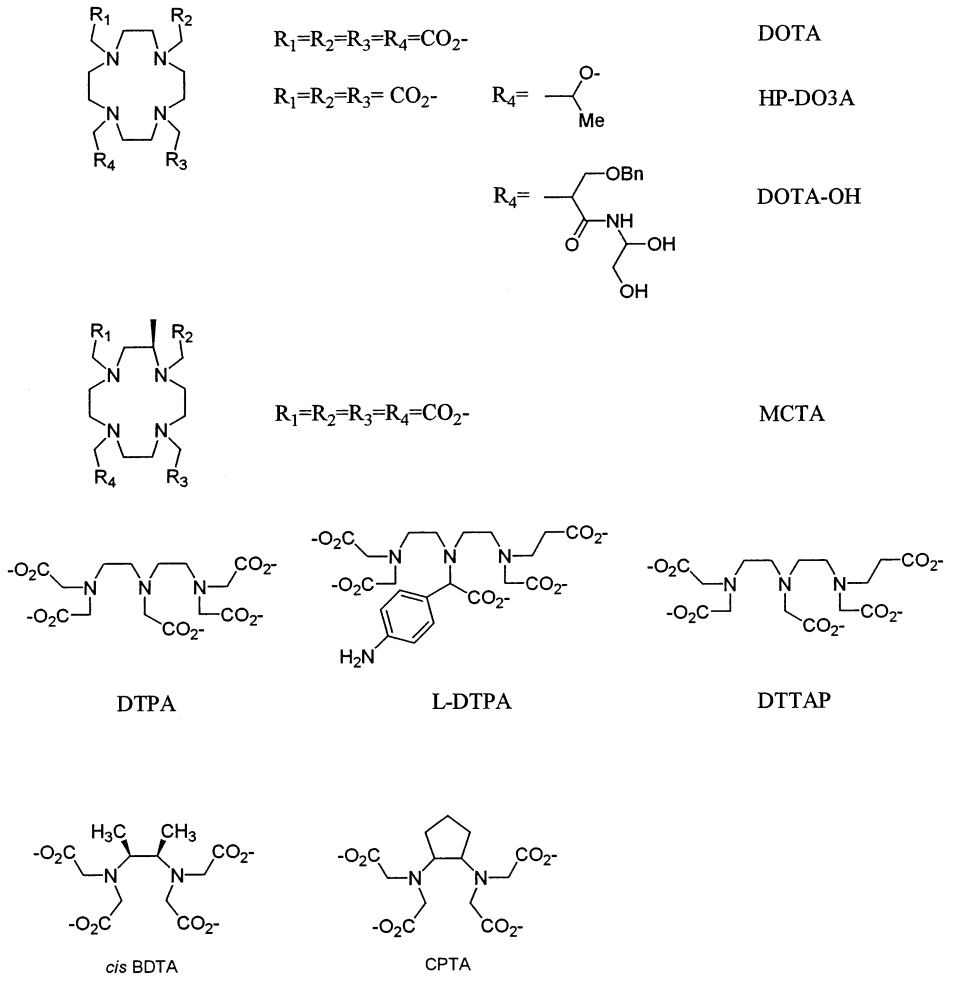

Fig. 8. Structures of ligands found to bind one water molecule ($q = 1$).

tions; electronic and electrostatic effects are not considered in this MM treatment.

Instead of dividing the Gd(III) complexes by type of ligand, such as EDTA or DTPA, the complexes were classified by the number of waters bound to the metal. Three main categories arise from this scheme, those with a hydration number of one; two; and three.

The majority of these complexes are derived from DTPA-type and DOTA-type parent ligands; structures of these ligands are found in Fig. 8. A total of 23 Gd(III) complexes were examined with the coordination scan and found to bind one water molecule. The majority of these complexes is eight-coordinate in terms of the ligand denticity, the binding of one water, then, brings the Gd(III) to a coordination number of nine.

Interestingly, when the thermodynamic stability constant log K is plotted against ΔE_{coord} (see Table 10), a linear correlation was discovered ($r^2 = 0.91$). This plot, shown in Fig. 9, clearly shows that this relationship between the stability and ΔE_{coord} is unaffected by the type of ligand, linear or macrocyclic. As ΔE_{coord} increases the thermodynamic stability decreases; this suggests that the rate-determining step of complex formation involves a reorganization of the essentially complete complex. The higher stability constants found for macrocyclic ligands suggests that this process is even more dominant, the ligand already exists in the binding conformation, and increasing the rigidity of the complex would, then, be expected to increase the stability by a larger extent than for a linear ligand. This effect can also be seen with two EDTA type ligands, which were found to bind only one water. The ligand CPTA is extremely rigid with a cyclopentyl ring incorporated within the ethylene bridge, while *cis* BDTA has two methyl groups on the backbone imparting rigidity.

A recent report suggested that an important factor affecting the proton relaxivity of lanthanide(III) complexes is the ability of the metal to pass through an intermediate with a coordination number of eight during the process of water exchange [49]. If this is indeed the case, the more rigid the ligand, the more difficult the change in the coordination state and, therefore, the lower the relaxivity. When the coordination scans were used to determine ΔE for this process, there was no correlation to the experimental relaxivities. It would appear that any effect is quite small and these subtle changes between ligands are easily overpowered by the rotational tumbling effects, which are dependent on the molecular mass.

As has been noted previously, Kumar and Tweedle [50] found an excellent correlation between the ligand strain energy, $E_{ML}-E_L$, and the complex stability in the case of polyaminomacrocycles. If we consider the energetic cost of reorganizing the complex from the solvated, maximum coordination, to the desolvated complex,

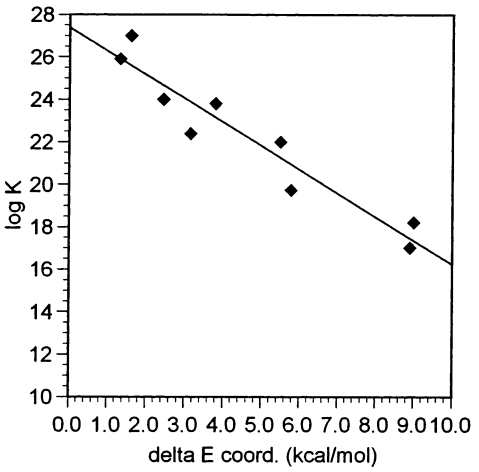

Fig. 9. Correlation of log K to ΔE_{coord} for gadolinium amino carboxylate complexes which bind one water molecule.

minimum coordination, as a measure of ligand rigidity, we would expect to find a correlation between ΔE_{coord} and the thermodynamic stability constant.

An exception to this trend are those ligands with amide groups involved in binding to the gadolinium which show a lower than expected stability. A reasonable explanation for this observation would be the difference in bond strengths between Gd(III) and an amide oxygen, compared to a carboxylate oxygen. In all of the bis(amide) complexes, two strong carboxylate–Gd interactions have been replaced by the weaker amide–Gd interaction with a commensurate drop in stability of ca. 10^5. All of the bis(amides) examined had an unsubstituted DTPA backbone, and the changes were all in the amide groups removed from the metal center; thus, one would expect these substitutions to play little role in rigidifying the complex.

4. Conclusions

We have found that molecular modeling can be extremely useful in designing and understanding the biological behavior of metal-based imaging agents. In order to utilize the power of molecular modeling fully with metals used in radiology, it will first be necessary to develop high quality parameter sets for these metals. We have made initial progress with parameters for Ga(III), In(III), Tc(V), and Gd(III), with many more elements awaiting parameterization. An important technique for designing ligands with high in vivo stability is the coordination scan. We have observed that if the metal coordinated by a particular ligand possesses vacant coordination sites, it frequently displays low in vivo stability. This technique has proved particularly valuable in understanding the behavior of gadolinium based MRI agents.

Acknowledgements

The authors wish to acknowledge financial support from the United States Department of Energy (DE-FG02-87ER60512) and the National Cancer Institute (CA-42925).

References

[1] I.D. Kuntz, E.C. Meng, B.K. Shoichet, Acc. Chem. Res. 27 (1994) 117–123.
[2] R.J. Boudreau, S.M.N. Efange, Invest. Radiol. 27 (1992) 653–658.
[3] S. Jurrison, D. Berning, W. Jia, D. Ma, Chem. Rev. 93 (1993) 1137–1156.
[4] G.R. Brubaker, D.W. Johnson, Coord. Chem. Rev. 53 (1984) 1–36.
[5] R.D. Hancock, Prog. Inorg. Chem. 37 (1989) 187–291.
[6] B.P. Hay, Coord. Chem. Rev. 126 (1993) 177–236.
[7] P. Comba, Coord. Chem. Rev. 123 (1993) 1–48.
[8] P. Comba, T.W. Hambley, Molecular Modeling of Inorganic Compounds, VCH Publishers, New York, NY, 1995.

[9] L. Hansen, R. Cini, A.J. Taylor, L.G. Marzilli, Inorg. Chem. 31 (1992) 2801–2808.
[10] R.J. Boudreau, S.C. Jackels, S.M.N. Efange, H.F. Kung, J. Nucl. Med. 35 (1994) 243P.
[11] A.A. Vitale, M.A. Calviño, C.C. Ferrari, A.E. Stahl, A.B. Pomilio, J. Label. Compd. Radiopharm. 36 (1995) 509–519.
[12] R.J. Boudreau, J.E. Mertz, Nucl. Med. Biol. 24 (1997) 395–398.
[13] Y. Sun, C.J. Anderson, T.S. Pajeau, D.E. Reichert, R.D. Hancock, R.J. Motekaitis, A.E. Martell, M.J. Welch, J. Med. Chem. 39 (1996) 458–470.
[14] C.J. Anderson, C.S. John, Y.J. Li, R.D. Hancock, T.J. McCarthy, A.E. Martell, M.J. Welch, Nucl. Med. Biol. 22 (1995) 165–173.
[15] R.D. Hancock, D.E. Reichert, M.J. Welch, Inorg. Chem. 35 (1996) 2165–2166.
[16] D.E. Reichert, R.D. Hancock, M.J. Welch, Inorg. Chem. 35 (1996) 7013–7020.
[17] SYBYL 6.2 ed., Tripos Inc., St Louis, 1995.
[18] A.E. Martell, R.D. Hancock, Metal Complexes in Aqueous Solutions, Plenum Press, New York, 1996.
[19] R.D. Shannon, Acta Crystallogr. Sect. A 32 (1976) 751–767.
[20] Y. Li, A.E. Martell, R.D. Hancock, J.H. Reibenspies, C.J. Anderson, M.J. Welch, Inorg. Chem. 35 (1996) 404–414.
[21] J.A. Katzenellenbogen, J. Nucl. Med. 36 (1995) 8S–13S.
[22] R.K. Hom, D.Y. Chi, J.A. Katzenellenbogen, J. Org. Chem. 61 (1996) 2624–2631.
[23] K.E. Baidoo, U. Scheffel, S.Z. Lever, M. Stathis, H.N. Wagner, J. Nucl. Med. 36 (1995) 28P.
[24] B. Johannsen, M. Scheunemann, H. Spies, P. Brust, J. Wober, R. Syhre, H.-J. Pietzsch, Nucl. Med. Biol. 23 (1996) 429–438.
[25] D.Y. Chi, J.P. O'Neil, C.J. Anderson, M.J. Welch, J.A. Katzenellenbogen, J. Med. Chem. 37 (1994) 928–937.
[26] K.E. Baidoo, S.Z. Lever, U. Scheffel, Bioconjugate Chem. 5 (1994) 114–118.
[27] A. Davison, A.G. Jones, J. Appl. Radiat. Isotopes 33 (1982) 875–881.
[28] G. Bandoli, U. Mazzi, E. Roncari, E. Deutsch, Coord. Chem. Rev. 44 (1982) 191.
[29] A.K. Rappé, K.S. Colwell, C.J. Casewit, Inorg. Chem. 32 (1993) 3438–3450.
[30] J. Kornyei, I. Szilvasi, Z. Nagy, I. Foldes, Izotoptech. Diagn. 37 (1994) 221–223.
[31] S.M. Nikitin, V.N. Kulakov, Radiochemistry (Moscow) 39 (1997) 398–401 Translation of Radiokhimiya.
[32] R. Gonzalez, C. Kremer, R. Chiozzone, J. Torres, M. Rivero, A. Leon, E. Kremer, Radiochim. Acta 81 (1998) 207–213.
[33] M. Neves, R. Fausto, Nucl. Med. Biol. 26 (1999) 85–89.
[34] S.A. Zuckman, G.M. Freeman, D.E. Troutner, W.A. Volkert, R.A. Holmes, D.G. Van Derveer, E.K. Barefield, Inorg. Chem. 20 (1981) 2386–2389.
[35] H.J. Weinmann, R.C. Brasch, W.R. Press, G.E. Wesbey, Am. J. Roentgenol. 142 (1984) 619–624.
[36] W.P. Cacheris, S.C. Quay, S.M. Rocklage, Magn. Reson. Imaging 8 (1990) 467–481.
[37] R. Fossheim, S.G. Dahl, Acta Chem. Scand. 44 (1990) 698–706.
[38] R. Fossheim, H. Dugstad, S.G. Dahl, J. Med. Chem. 34 (1991) 819–826.
[39] R. Fossheim, H. Dugstad, S.G. Dahl, Eur. J. Med. Chem. 30 (1995) 539–546.
[40] B.P. Hay, Inorg. Chem. 30 (1991) 2876–2884.
[41] T.R. Cundari, E.W. Moody, S.O. Sommerer, Inorg. Chem. 34 (1995) 5989–5999.
[42] B.P. Hay, O. Clement, G. Sandrone, D.A. Dixon, Inorg. Chem. 37 (1998) 5887–5894.
[43] A.K. Rappé, C.J. Casewit, K.S. Colwell, W.A.I. Goddard, W.M. Skiff, J. Am. Chem. Soc. 114 (1992) 10024–10035.
[44] U. Cosentino, G. Moro, D. Pitea, A. Villa, P.C. Fantucci, A. Maiocchi, F. Uggeri, J. Phys. Chem. A 102 (1998) 4606–4614.
[45] K. Hegetschweiler, R.D. Hancock, M. Ghisletta, T. Kradolfer, V. Gramlic, H.W. Schmalle, Inorg. Chem. 32 (1993) 5273–5284.
[46] N. Govindaswamy, D.A. Quarless, Jr, S.A. Koch, J. Am. Chem. Soc. 117 (1995) 8468–8469.
[47] C.S. Cutler, M.C. Giron, D.E. Reichert, A.Z. Snyder, P. Herrero, C.J. Anderson, D.A. Quarless, S.A. Koch, M.J. Welch, Nucl. Med. Biol. 26 (1999) 305–316.

[48] R.J. Motekaitis, A.E. Martell, S.A. Koch, J. Hwang, D.A.J. Quarless, M.J. Welch, Inorg. Chem. 37 (1998) 5902–5911.
[49] D. Pubanz, G. González, D.H. Powell, A.E. Merbach, Inorg. Chem. 34 (1995) 4447–4453.
[50] K. Kumar, M.F. Tweedle, Inorg. Chem. 32 (1993) 4193–4199.
[51] D.A. Moore, P.E. Fanwick, M.J. Welch, Inorg. Chem. 28 (1989) 1504–1506.
[52] U. Bossek, D. Hanke, K. Wieghardt, Polyhedron 12 (1993) 1.
[53] L. Templeton, D.H. Templeton, A. Zalkin, H.W. Ruben, Acta Crystallogr. Sect. B 38 (1982) 2155–2159.
[54] H. Gries, H. Miklautz, Physiol. Chem. Phys. Med. NMR 16 (1984) 105–112.
[55] S. Aime, M. Botta, M. Fasano, S. Paoletti, P.L. Anelli, F. Uggeri, M. Virtuani, Inorg. Chem. 33 (1994) 4707–4711.
[56] M.S. Konigs, W.C. Dow, D.B. Love, K.N. Raymond, S.C. Quay, S.M. Rocklage, Inorg. Chem. 29 (1990) 1488–1491.
[57] C.F.G.C. Geraldes, A.M. Urbano, M.A. Hoefnagel, J.A. Peters, Inorg. Chem. 32 (1993) 2426–2432.
[58] F. Uggeri, S. Aime, P.L. Anelli, M. Botta, M. Brochetta, C. de Haën, G. Ermondi, M. Grandi, P. Paoli, Inorg. Chem. 34 (1995) 633–642.
[59] C.A. Chang, L.C. Francesconi, M.F. Malley, K. Kumar, J.Z. Gougoutas, M.F. Tweedle, D.W. Lee, L.J. Wilson, Inorg. Chem. 32 (1993) 3501–3508.
[60] S.I. Kang, R.S. Ranganathan, J.E. Emswiler, K. Kumar, J.Z. Gougoutas, M.F. Malley, M.F. Tweedle, Inorg. Chem. 32 (1993) 2912–2918.
[61] S. Aime, P.L. Anelli, M. Botta, F. Fedeli, M. Grandi, P. Paoli, F. Uggeri, Inorg. Chem. 31 (1992) 2422–2428.
[62] K. Kumar, C.A. Chang, L.C. Francesconi, D.D. Dischino, M.F. Malley, J.Z. Gougoutas, M.F. Tweedle, Inorg. Chem. 33 (1994) 3567–3575.
[63] S.W.A. Bligh, N. Choi, E.G. Evagorou, M. McPartlin, W.J. Cummins, J.D. Kelly, Polyhedron 11 (1992) 2571–2573.